5715169

POPULAR SUMMARY
HJZ, August 15, 2001

Analysis of GPS data collected on the Greenland ice sheet

K. Larson, J. Plumb, J. Zwally, and W. Abdalati

This paper describes methods for analyzing GPS data at moving locations on the Greenland ice sheet and is not of direct popular interest.

Submitted to Polar Geography Ver 2

Analysis of GPS data collected on the Greenland ice sheet

Kristine Larson and John Plumb

Department of Aerospace Engineering Sciences, University of Colorado, Boulder

Jay Zwally

NASA Goddard Space Flight Center

Waleed Abdalati

NASA Headquarters, Washington D.C.

Short title: GPS AT THE SWISS CAMP

Abstract. For several years, GPS observations have been made year round at the Swiss Camp, Greenland. The GPS data are recorded for 12 hours every 10-15 days; data are stored in memory and downloaded during the annual field season. Traditional GPS analysis techniques, where the receiver is assumed not to move within a 24 hour period, is not appropriate at the Swiss Camp, where horizontal velocities are on the order of 30 cm/day. Comparison of analysis strategies for these GPS data indicate that a random walk parameterization, with a constraint of 1-2 10^{-7} km/sqrt(sec) minimizes noise due to satellite outages without corrupting the estimated ice velocity. Low elevation angle observations should be included in the analysis in order to increase the number of satellites viewed at each data epoch. Carrier phase ambiguity resolution is important for improving the accuracy of receiver coordinates.

1. Introduction

GPS observations on the Greenland ice sheet are generally restricted to campaign style measurements made during the summer field season. By comparison of measurements made in different years, the velocity of locations on the ice sheet can be determined with a precision of better than 10 cm/yr [*Thomas et al.*, 2000]. While annual GPS measurements are extremely useful, the ice flow velocity estimates extracted from these observations assume that velocity is constant throughout the year. In order to investigate the variability of ice flow velocities, continuous or quasi-continuous GPS measurements are required. While continuous GPS measurements have been made in Greenland since 1995, the receivers have been generally on bedrock rather than the ice (Figure 1). These sites were installed for investigations of solid Earth phenomena and/or support of GPS orbit determination. The horizontal motions of the bedrock sites are on the order of 1 cm/yr, which is consistent with the predictions of global plate motions for North America [*Argus and Gordon*, 1991]. There is generally little significant non-linear motion at permanent bedrock sites in Greenland [*van Dam et al.*, 2000].

The speed of ice flow in Greenland is 3-4 orders of magnitude larger than tectonic motions observed on bedrock, depending on where you make your observations [*Thomas et al.*, 2000]. Unlike tectonic motions, which are generally steady, it is not clear that surface velocities at different locations on the

icean sheet are or should be constant. Observations of interannual variations in ice flow velocities would provide valuable insight about the flow characteristics that may be linked to seasonal parameters.

In 1996 an experiment was begun to measure variations in ice flow velocity near the Swiss Camp (Figure 1). Established in 1990 at the nominal equilibrium line, the Swiss Camp has provided an extensive record of climatological variables and input for energy balance models [*Steffen and Box*, in press]. Because the equilibrium line is the boundary between areas of net mass gain (accumulation) and net mass loss (ablation), ice sheet behavior in this vicinity is of great interest. Morever, the existing infrastructure and extensive ancillary data make the site particularly well-suited for a geodetic study of the ice sheet.

2. Installation at Swiss Camp

A dual frequency GPS antenna was mounted on a 4-meter long (0.09 m outer diameter) pole which was placed into a 2-meter deep hole that was drilled into the ice. This left 2 meters extending above the ice (Figure 2) to ensure that the antenna would remain above any snow accumulation that would occur during the measurement period. Snow accumulation was typically between 1 and 1.5 meters. The pole was aligned vertically using a level and then frozen into the ice for stability. Attached to the top of the pole is a specially designed leveling/mounting device that allows for easy leveling and orientation of the antenna; it is made very secure once the antenna is mounted. The receiver was placed inside an insulated protective box about 4 m from the antenna. The system was powered by 4 to 6 batteries and connected to two 18 W solar panels.

While satellite communication is possible at the Swiss Camp, power consumption for transmitting the GPS data would be much greater than capabilities that existed when this project began. Thus the GPS data were stored in the receiver's memory and were recovered during the annual field season in May-June. Likewise, while the GPS receiver used in this project is capable of continuous observations, there was not sufficient power and storage space available; instead quasi-continuous measurements were made, at intervals that will be discussed below. A Trimble 4000 SSi unit was purchased and upgraded

from 5 to 40 Mbytes of internal memory so that an entire field seasons' results could be stored in it. Many geodetic GPS users cover antennas with plastic dome to avoid build-up of snow (and dirt) on the antenna element. A protective dome was not installed at the Swiss Camp because wind is sufficient to remove snow from the antenna. The GPS receiver was programmed to make observations for 12 hours at regular intervals. The spacing and length of the surveys was limited by availability of sunlight to power the batteries as well as internal memory to store the measurements. Winter measurements were made at 15-day intervals, while measurements the rest of the year were made at 10-day intervals.

Although the typical signal Swiss Camp velocity is much larger than most of the limiting error sources in GPS, the receiver was programmed in such a way to eliminate the effects of two particular error sources: constellation geometry and multipath. The GPS satellites have ground tracks that repeat with a sidereal period. In other words, an identical constellation is in view 23 hrs 56 minutes after the first measurements. In practice, some satellites might not be available from day to day because that satellite might be turned off or maneuvered by the Department of Defense. Synchronizing the observations also helps for reducing the error due to multipath. While the multpath error is not eliminated by synchronizing measurements, its impact is reduced because the same multipath environment should be seen from day to day.

Which 12 hours of data should be collected during each 24 hour period? Generally a time period with good constellation coverage should be used. One measure of optimal GPS tracking is position dilution of precision (PDOP), which is defined as:

$$\sqrt{\sigma_x^2 + \sigma_y^2 + \sigma_z^2} \tag{1}$$

where σ_x^2, σ_y^2, and σ_z^2 are the unweighted Cartesian coordinate variances [*Hoffmann-Wellenhof et al.*, 2001]. It is preferable to track satellites when PDOP values are small. Figure 3 shows PDOP for the Swiss Camp in July, 1998, with an annotation to denote which hours were used for this study. Note that this window avoided several large PDOP spikes earlier in the 24 hour period.

3. GPS Analysis

With the creation and expansion of the International GPS Service (IGS) [*Beutler et al.*, 1994], and its associated analysis centers, it has become far easier for polar scientists to use GPS for precise applications such as the one described in this paper. The IGS uses a global tracking network to estimate very precise GPS orbits and Earth orientation parameters. This network is also used to determine precise coordinates which are used to define the International Terrestrial Reference Frame (ITRF97) [*Boucher et al.*, 1999]. Positions of the Swiss Camp were estimated with respect to ITRF97.

The GPS observations from Swiss Camp were analyzed using the GIPSY software developed at the Jet Propulsion Laboratory (JPL) [*Lichten and Borders*, 1987]. Both the pseudorange and carrier phase data are used in GIPSY solutions, although the precision of the coordinate estimates are controlled by the more precise carrier phase observations. The carrier-phase and pseudorange observables, ($\Delta\phi_r^s$ and P_r^s) for a given satellite s and receiver r can be written as:

$$-\Delta\phi_r^s\lambda = \rho_g - c\delta^s + c\delta_r + N_r^s\lambda + \rho_t - \rho_i + +\epsilon_\phi \tag{2}$$

and

$$P_r^s = \rho_g - c\delta^s + c\delta_r + \rho_t + \rho_i + \epsilon_p \tag{3}$$

where λ is the carrier wavelength; ρ_g is the geometric range, defined as $|\vec{X}^s - \vec{X}_r|$; $\vec{X}^s$ is the satellite position at the time of signal transmission; $\vec{X}_r$ is the receiver position at reception time; δ_r and δ^s are the receiver and satellite clocks, respectively; ρ_t and ρ_i are the propagation delays due to the troposphere and ionosphere; N_r^s is the carrier-phase ambiguity or bias. Included in N_r^s are phase delay terms originating in the receiver and the satellite transmitter; c is the speed of light. ϵ_p and ϵ_ϕ are noise terms for the pseudorange and carrier phase observables, respectively. For simplicity, multipath errors are not shown.

While the receiver produced observations at 15 second intervals, the data were later decimated to 5 minute intervals to reduce the computational burden. This is appropriate when receiver motions (on the order of cm/hr) are small compared to the observation period (5 minutes). The 15 second data are

extremely helpful for resolving cycle slips, which are particularly problematic at high latitudes. Data from the two GPS frequencies, L_1 and L_2, are combined to remove most of the effects of the ionosphere (ρ_i). Along with the data from Swiss Camp, data from the other sites in Greenland (Figure 1) were also analyzed, although the positions of these sites were not allowed to vary with time.

The GPS parameter estimation strategy used is summarized in Table 1. The constraints used for the carrier phase ambiguities, clocks, and troposphere (N_r^s, δ_r, δ^s, and ρ_t) are identical to those used for global plate motion [*Larson et al.*, 1997] and time-transfer studies [*Larson and Levine*, 1999] except for the treatment of Swiss Camp's coordinates. The satellite orbits ($\vec{X}^s$) and Earth orientation parameters were fixed to values provided by the IGS and the International Earth Rotation Service, respectively.

We also investigated the possibility of using JPL's precise point positioning technique [*Zumberge et al.*, 1997]. This analysis strategy has the advantage that only the data from Swiss Camp need to be analyzed. A major disadvantage is that the resulting solution does not allow for ambiguity resolution [*Blewitt*, 1989], which requires data from two or more GPS receivers. In a later section, we will demonstrate the importance of ambiguity resolution in estimating time-varying station coordinates.

4. Receiver Coordinates

In many geophysical applications it can be assumed that GPS receivers do not move during the 24 hour observing period. This is clearly not the case on active volcanoes [*Owen et al.*, 2000] and ice sheets. In principle it is simple to vary receiver coordinates in GIPSY, which allows time-varying processes to be modeled as a "white noise" process, with no temporal correlation, a random walk process with infinite correlation, or with more general Gauss-Markov processes with intermediate correlation lengths. Results were compared using different correlation lengths; they were found to be no more precise or accurate than a random walk model, so the focus of this paper is the random walk model. For comparison, white noise coordinate estimates were also estimated.

For a random walk the position of the GPS receiver, x, is defined:

$$x_{k+1} = x_k + w_k \tag{4}$$

where w is random noise and the indices $k+1$ and k refer to increments in time. The noise covariance q_k is:

$$q_k = q(t_{k+1} - t_k) = q\Delta t \tag{5}$$

q then is the variance per unit time and generates the random walk [*Technical Staff*, 1974]. In the GIPSY software, $\sqrt{q}$ is an input; the units of this parameter are $km/\sqrt{sec}$. Following the GIPSY notation, $\sqrt{q}$ will be referred to as σ_{rw}; the units will always be defined as above.

A value of σ_{rw} needs to be chosen which is appropriate for the time scales found in the data. One must first assess how much the positions vary in time. For many geophysical applications, temporal variability is small, e.g. positions move 0.1 to 10 cm/hr. A σ_{rw} value for these time scales should be chosen in such a way as to minimize noise in the estimates. If σ_{rw} is too small, the position estimates will be biased towards no motion. In any case, a σ_{rw} chosen for slow moving geophysical applications would not be appropriate for other GPS filtering applications, such as for data collected on a moving aircraft. In the latter case, white noise estimation would be appropriate.

5. Analysis and Discussion of Scoresbysund Data

The selection of the optimal σ_{rw} value for Swiss Camp is complicated by the fact that while the ice is moving, we do not know its velocity exactly and we cannot be sure that the velocity in summer, for example, is the same as the velocity in winter. Ideally we would like to test our filtering strategy on a data set collected with the same satellite geometry as Swiss Camp but with exact knowledge of how fast the receiver (or ice) moved. Scoresbysund (Figure 1) is ideally located for testing Swiss Camp filtering strategies. Scoresbysund (70.48 degrees) is at a similar latitude as Swiss Camp (69.57 degrees). Unlike Swiss Camp, it is continuously operating and can be used to assess the impact of "data quality" on position estimates over an entire year.

Figure 4 is indicative of data quality problems associated with high latitude sites. The number of observations collected for a year are plotted for two sites: Scoresbysund and Table Mountain, Colorado (40.13 degrees). While the mean number of observations used in the Scoresbysund solution is significantly higher than at Table Mountain, this simply reflects that a 12 channel receiver has been installed at Scoresbysund, and the Table Mountain receiver is an older model 8 channel receiver. The number of channels relates to the number of satellites that can be tracked at any given time. The Table Mountain receiver tracks fewer satellites, but it does so much more consistently. The slight change in observations around day 120 is the result of adding a new GPS satellite (PRN08) to the solution. Although this satellite was launched in late 1997, several months pass before a new satellite is declared operational and used in IGS orbit solutions.

The GPS antenna at Scoresbysund has been installed on bedrock and should move less than 0.1 mm in a 24 hour period. While we could investigate the ability to measure null velocities at Scoresbysund, the filtering strategy could be inadvertently biased, i.e. a small σ_{rw} could produce a velocity of 0 cm/hr, but not a larger velocity like 1 cm/hr. *Elosegui et al.* [1996] built an apparatus that moved a GPS antenna at a predefined velocity, 1 mm/hr, and then varied their filtering strategy to see which best recovered the given antenna velocity. Alternative filtering strategies can be tested using observations from Scoresbysund with a simulated *a priori* velocity. In each case, the *a priori* receiver position is defined to move horizontally by 30 cm/day. When the receiver position is subsequently estimated, it should move at a velocity which is the negative of the input velocity, since the Scoresbysund receiver didn't actually move.

Several Scoresbysund solutions have been highlighted in Figure 4. These will be used to illustrate some of the features in the data, particularly as they relate to data quality and varying filtering strategies. In each case the number of visible satellites above a 10 degree elevation cutoff is shown. An *a priori* velocity of 30 cm/day was input into the horizontal receiver coordinates, and subsequently that same signal was removed so that the residual position estimates could be inspected (Figure 5). σ_{rw} was set to 10^{-7} km/sqrt(sec). The two numerical solutions shown used different elevation angle

cut-offs. For many years a 15 degree cutoff was used in many geodetic analyses [*Lichten and Border*, 1987; *Blewitt*, 1989], although others used even higher cutoffs, e.g. 20 degrees [Bernese reference]. Most cycle slips occur at lower elevation angles, and the data are, in general, noisier because of multipath. It is also more difficult to accurately correct the tropospheric delay at the lower elevation angles. For all these reasons, lower elevation data are frequently discarded. Subsequent work has shown that a more reliable vertical estimate can be determined by using lower elevation angle data [*Bar Sever et al.*, 1998]. This was also the case for the kinematic simulation for Scoresbysund. Inclusion of the lower elevation angle data has little influence on the horizontal velocities but has a pronounced impact on the vertical velocity. The slope of the vertical displacement (bottom panel of Figure 5) is reduced from -3.4 cm/day to -0.2 cm/day by using an elevation angle cutoff of 10 degrees, which significantly improves the agreement with the *a priori* velocity of 0 cm/day.

The top panel of Figure 5 shows a significant data outage in the first 3 hours of data. This could be a real satellite outage or could be related to the quality of receiver tracking on July 5. PDOP is shown in Figure 6 for both the actual number of satellites that were broadcasting on that day and the satellites observed by Scoresbysund. It is apparent that the receiver had great difficulty tracking at approximately 01:00 UTC. This will, in general, result in poorer ability to resolve position and velocity.

Figure 7 shows Scoresbysund solution results for November 8. On this particular day there were approximately 20% fewer observations than on July 5, with most of the data outage concentrated in the first 6 hours of the data file. Again, the north component gives a fairly robust estimate of velocity, but there is a significant transient observed in the east component which is directly related to the satellite outages in the early part of the day. For most locations on the Earth, the GPS satellites track preferentially north-south which leads to weaker estimates of the east component, particularly when few satellites are in view.

Assuming that a sufficient number of satellites are available, we still have not resolved the issue of choosing an optimal value of σ_{rw}. The impact of varying σ_{rw} in the time domain is shown in Figure 8. For the white noise case, equivalent to a large σ_{rw} value, one can see that satellite outages have a

enormous impact. As σ_{rw} is decreased, the noise features also become smaller. The tighter random walk constraints also produce more reasonable solutions during satellite outages. If the σ_{rw} constraint is tightened too much, the estimated velocity can significantly deviate from the input velocity. The Scoresbysund filter test cases are summarized in Figure 9. In each case solutions were computed for σ_{rw}'s that vary by nearly three orders of magnitude. The solutions for very small σ_{rw}, e.g. 10^{-9}, incorrectly estimate a velocity of 0 cm/day. An accurate solution, 30 cm/day, is recovered at values at 710^{-8} and above.

Each of the cases discussed above used 24 hours to resolve velocity. Because of memory and power limitations, only 12 hours of GPS data will be available at the Swiss Camp. It would be useful to determine how much data would be required to estimate an accurate velocity. In Figure 10 solutions are computed for three values of σ_{rw}, 710^{-8}, 10^{-7}, and 310^{-7}. The solutions are also computed using different lengths of time, ranging from 3-24 hours. Again, the north component needs fewer data to correctly estimate the input velocity of 30 cm/day; the east component results suggest our observing period should have been a little longer than 12 hours, with converged solutions at 15 hours. We can use the misfit so as to properly estimate the velocity uncertainties computed for Swiss Camp.

In each of the cases shown above, the solutions were bias fixed (N_r^s). This is also known as ambiguity resolution. The value of ambiguity resolution for static GPS applications has been long established [*Blewitt,* 1989; *Dong and Bock,* 1989] and it would be unexpected if ambiguity resolution didn't improve the position estimates. For the sake of completeness, GPS position estimates at Scoresbysund are shown in Figure 11, with and without ambiguity resolution. Clearly the filter solution for the east and vertical bias free solution disagrees markedly with the *a priori* input, with little effect on the north component.

6. Analysis and Discussion of Swiss Camp Data

As noted previously, the Swiss Camp receiver was programmed to operate at regular intervals throughout the year, with more frequent operation in the spring-summer-fall. The number of usable

observations is shown in Figure 12, for both 10 and 15 degree elevation angle cutoffs. Data retrieval was fairly good, with only one day of observations lost due to complete receiver failure. On two days the receiver stopped tracking after 3-4 hours; we will not report results for these days. On three days it appears that no data below 15 degrees were tracked by the receiver. After searching the database, it was discovered that on those three days the field crew inadvertently programmed the receiver to *not* track below 15 degrees.

As at Scoresbysund, occasional data outages were observed at data collected at the Swiss Camp. The Swiss Camp solutions for August 4, 1998 are shown in Figure 13. By comparing with data collected only two weeks earlier, the satellites outages on August 4 can be clearly discerned. The impact of the satellite outages on August 4 can be observed in the white noise position estimates shown in the bottom panels of Figure 13. Even with these data outages, a proper random walk estimation strategy (also shown in Figure 13) yields significantly smoother estimates, which agree well with estimates earlier in the day when a full constellation was tracked. The data outages on this day at Swiss Camp correspond to frequent lost of lock on the L2 frequency. There was no corresponding difficulty in tracking L2 on the other sites in Greenland on this day.

The coordinate results for one year of GPS data from the Swiss Camp are shown in north, east, and vertical coordinates in Figure 14. The direction of local ice flow motion can be determined by estimating the long-term trend in the east and north directions, with an average velocity of 31.8±0.1 cm/day. The Swiss Camp is also dropping vertically at a rate of 0.6±0.1 cm/day. After removing the linear trend from the position estimates, we can see the residual variation of Swiss Camp coordinates (Figure 15). These position estimates confirm that there are significant residuals in ice velocity that correlate with seasons. A discussion of the scientific implications of this temporal variability is beyond the scope of this paper, but can be found in *Zwally et al.* (in preparation).

7. Conclusions

It has been demonstrated that autonomous GPS systems can be successfully deployed on the Greenland ice sheet. In this experiment, solar cells and battery power were used to operate the equipment. Other investigators have tried to use wind power (in Antarctica), with much less success. The receiver appears to have operated with little difficulty in the extreme temperature environment.

Solutions computed at Scoresbysund demonstrate the value of tracking satellites at lower elevation angles. This suggests that older model receivers (8 channels) should not be used; newer models that can track up to 12 satellites will result in more robust solutions.

8. Acknowledgements

We thank Koni Steffen for logistical support at the Swiss Camp This research was supported by NASA grants to the University of Colorado and Goddard Space Flight Center. UNAVCO provided technical assistance. We thank UNAVCO, JPL, NGS, KMS, and BKG for supporting continuous GPS observations at Kulusuk (KULU), Thule (THU1), Kellyville (KELY), Scoresbysund (SCOB), and Reykjavik(REYK), respectively. Data for THU1, KELY, and REYK are freely available via anonymous ftp from the IGS (igscb.jpl.nasa.gov). Data from KULU and SCOB are available from UNAVCO (www.unavco.ucar.edu.) and the KMS (forskning.kms.dk), respectively.

References

Argus, D. and R. Gordon, No-net rotation model of current plate velocities incorporating plate motion model NUVEL-1, *Geophys. Res. Lett., 18*, 2039-2042, 1991.

Bar-Sever, Y. E., A new model for GPS yaw attitude, *Proc. IGS Workshop: Special Topics and New Directions*, edited by G. Gendt and G. Dick, GeoForschungsZentrum, Potsdam, Germany, pp. 128-140, 1996.

Bar Sever, Y., P Kroger, and J. Borjesson, Estimating horizontal gradients of tropospheric path delay with a single GPS receiver, *J. Geophys. Res., 103*, 5019-5035, 1998

Beutler, G., I.I. Mueller, and R.E. Neilan, The International GPS Service for Geodynamics (IGS): Development and start of official service on January 1, 1994, *Bull. Geod., 68*, 39-70, 1994.

Blewitt, G., Carrier phase ambiguity resolution for the Global Positioning System applied to geodetic baselines up to 2000 km, *J. Geophys. Res., 94*, 10,187-10,203, 1989.

Boucher, C., Z. Altamimi, and P. Sillard, The 1997 International Terrestrial Reference Frame (ITRF97), *IERS Tech. Note 27*, Int. Earth Rotation Serv., Paris, 1999.

Dong, D. and Y. Bock, Global Positioning System network analysis with phase ambiguity resolution applied to crustal deformation studies in California, *J. Geophys. Res., 94*, 1989.

Elosegui, P., J. Davis, J. Johansson, and I. Shapiro, Detection of transient motions with the Global Positioning System, *J. Geophys. Res.*, 101, 11,249-11,261, 1996.

Hoffman-Wellenhof, *GPS: Theory and Practice*, fifth edition, Springer-Verlag, 2001.

Larson, K.M., J. Freymueller and S. Philipsen, Global Plate Velocities from the Global Positioning System, *J. Geophys. Res., 102*, 9961-9982, 1997.

Larson, K.M. and J. Levine, Carrier Phase Time Transfer, *IEEE Trans. on Ultrasonics, Ferroelectronics, and Frequency Control, Vol.46,* 1001-1012, 1999.

Lichten, S. and J. Border, Strategies for high precision GPS orbit determination, *J. Geophys. Res., 92*, 12,751-12,762, 1987.

Owen, S., P. Segall, M. Lisowski, M. Murray, M. Bevis, and J. Foster, The January 30, 1997 eruptive event on Kilauea Volcano, Hawaii, as monitored by continuous GPS, *Geophys. Res. Lett., 27*, 2757-2560, 2000.

Steffen, K., and J. Box, Surface climatology of the Greenland ice sheet: Greenland climate network 1995-1999, *J. Geophys. Res.*, in press.

Technical Staff, The Analytic Sciences Corporation, *Applied Optimal Estimation,* ed. Arthur Gelb, The MIT Press, Cambridge, MA, 1974.

Thomas, R., T. Akins, B. Csatho, M. Fahnestock, P. Gogineni, C. Kim and J. Sonntag, Mass Balanace of the Greenland ice sheet at high elevations *Science, 289(5478)* 426-428, 2000.

van Dam, T., J. Wahr, K. Larson, O. Francis, and S. Gross, Using Geodesy to Observe Ice Mass Changes, *EOS*, Vol. 81, No. 37, 421-427, 2000.

Zumberge, J.F., M.B. Heflin, D.C. Jefferson, M.M Watkins, and F.H. Webb, Precise point positioning for the efficient and robust analysis of GPS data from large networks, *J. Geophys. Res., 102*, 5005-5017, 1997.

Zwally, H. J., W. Abdalati, K. Larson, and K. Steffen, Melt-Induced acceleration of Greenland Ice Sheet flow, manuscript in preparation.

Received _____

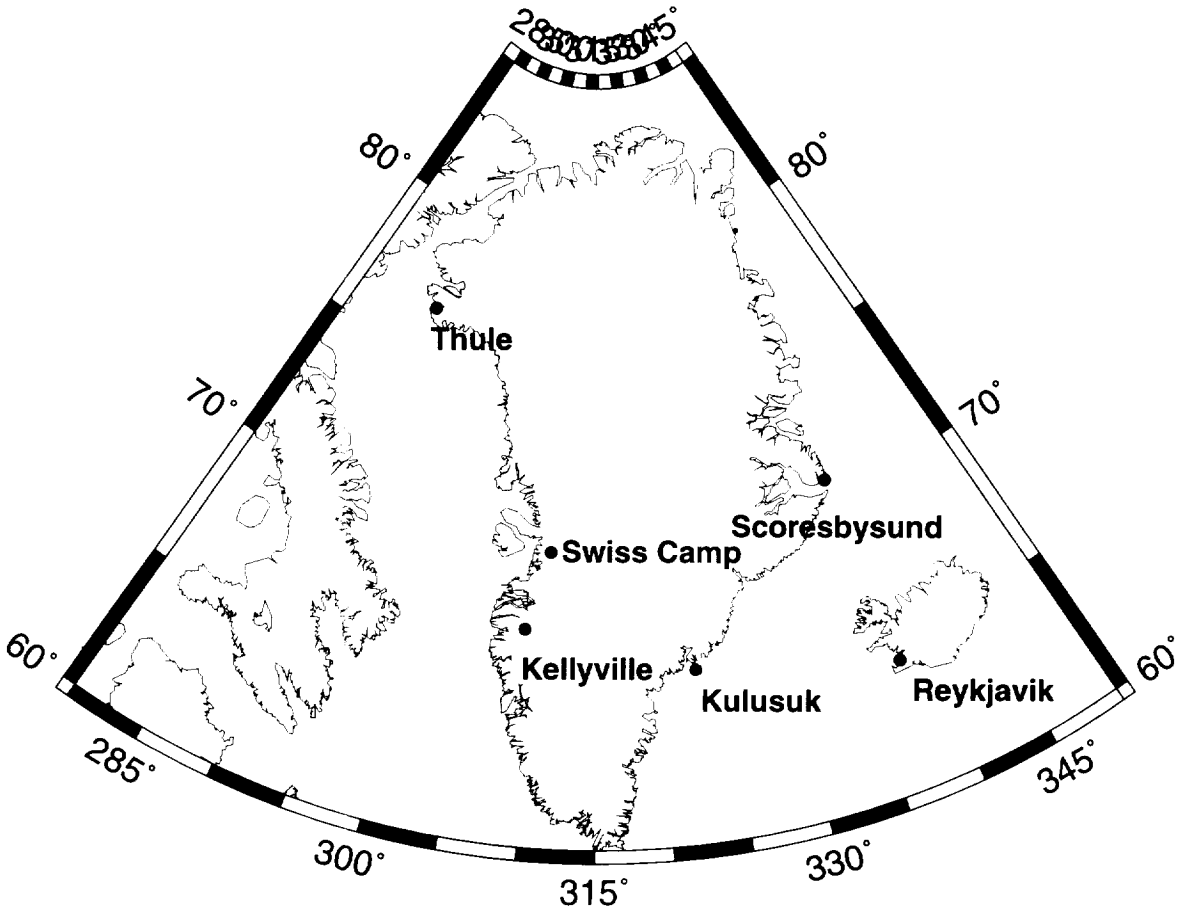

Figure 1. Continuously operating GPS sites in Greenland and Iceland.

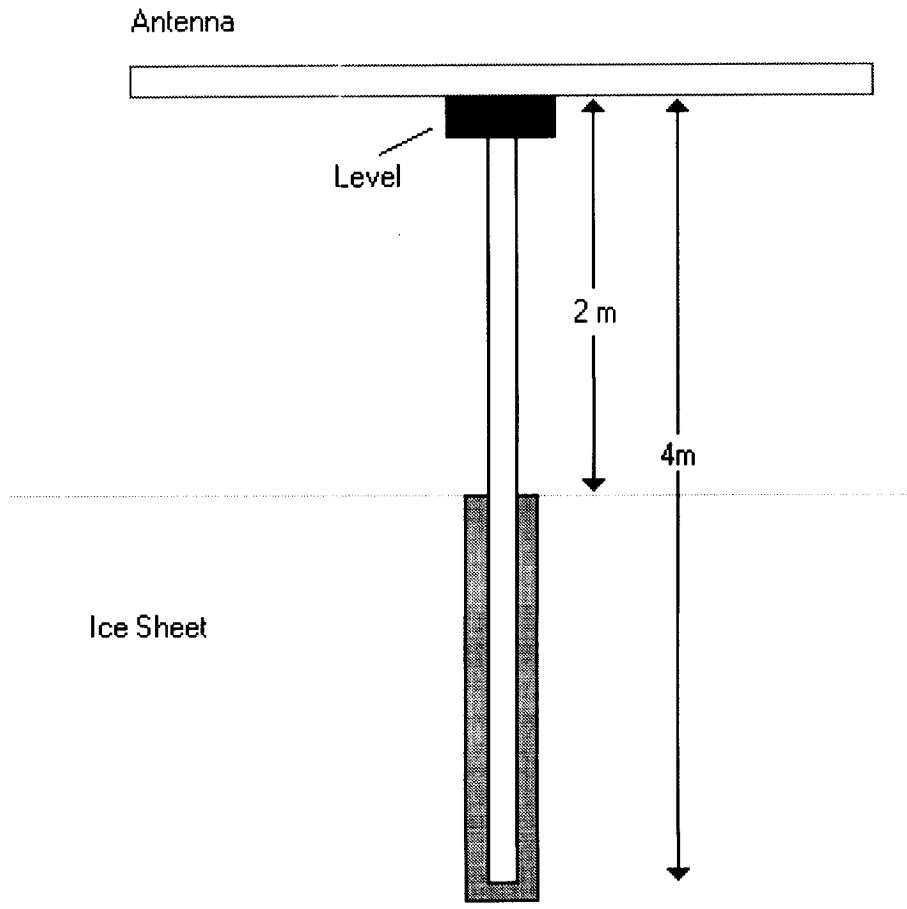

Figure 2. The antenna installation at Swiss Camp.

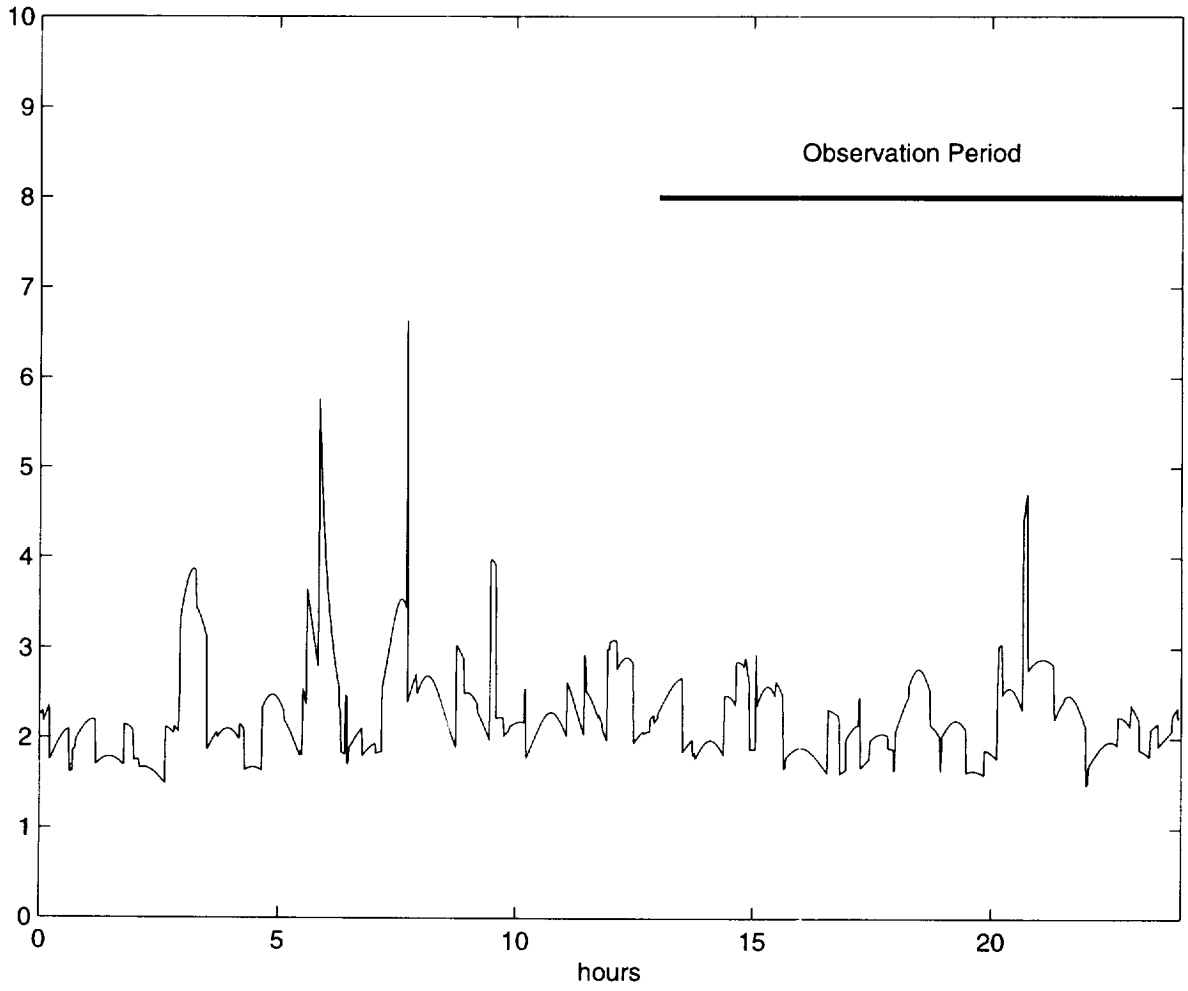

Figure 3. PDOP for all satellites above an elevation cut-off of 10 degrees at the Swiss Camp, 1998-JUL-05.

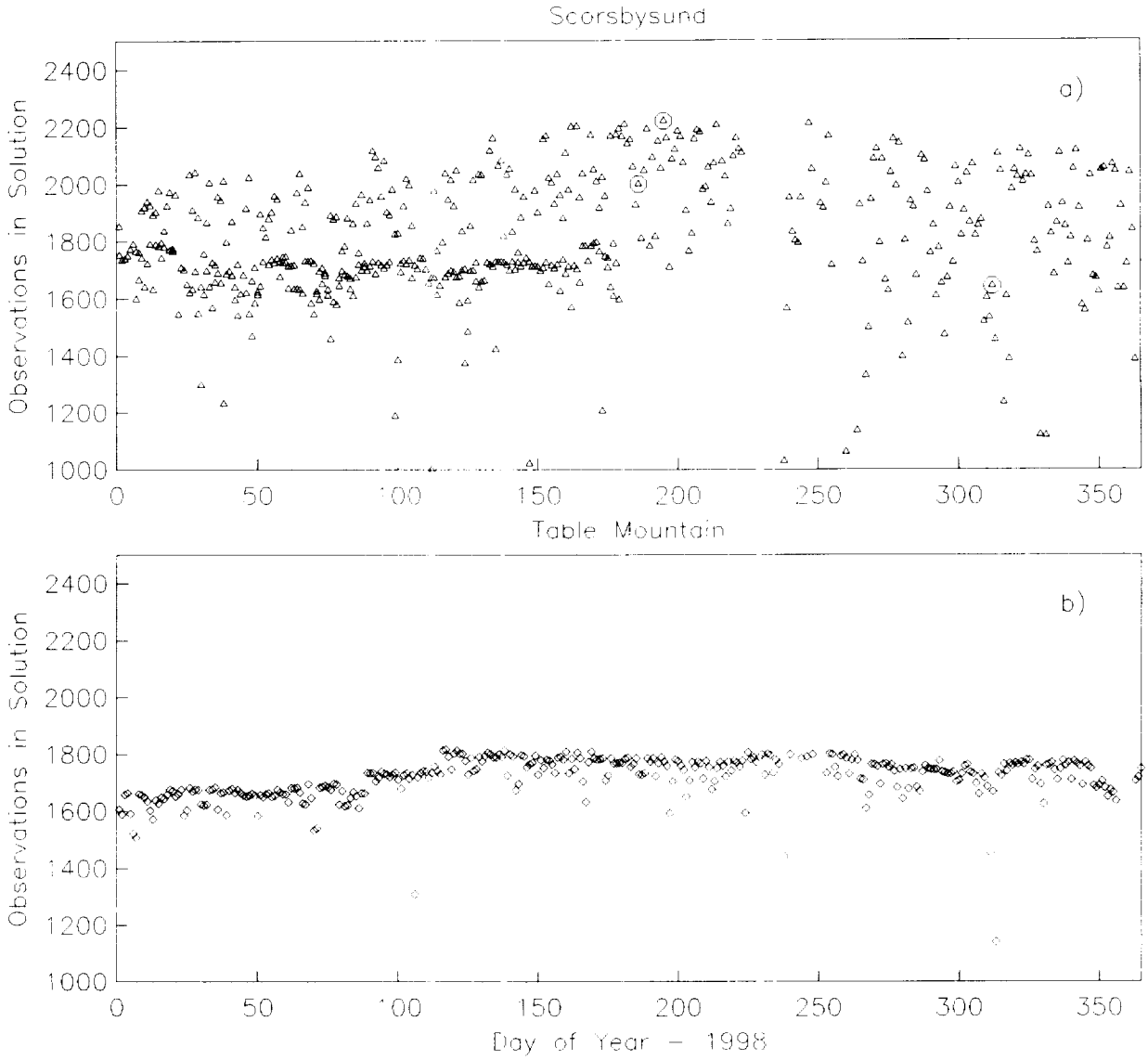

Figure 4. Number of observations used in a 24 hour GIPSY solution for Scoresbysund and Table Mountain. Scoresbysund is located at a latitude of 70.48; Table Mountain is located at a latitude of 40.13. Three days are circled and are discussed in the text.

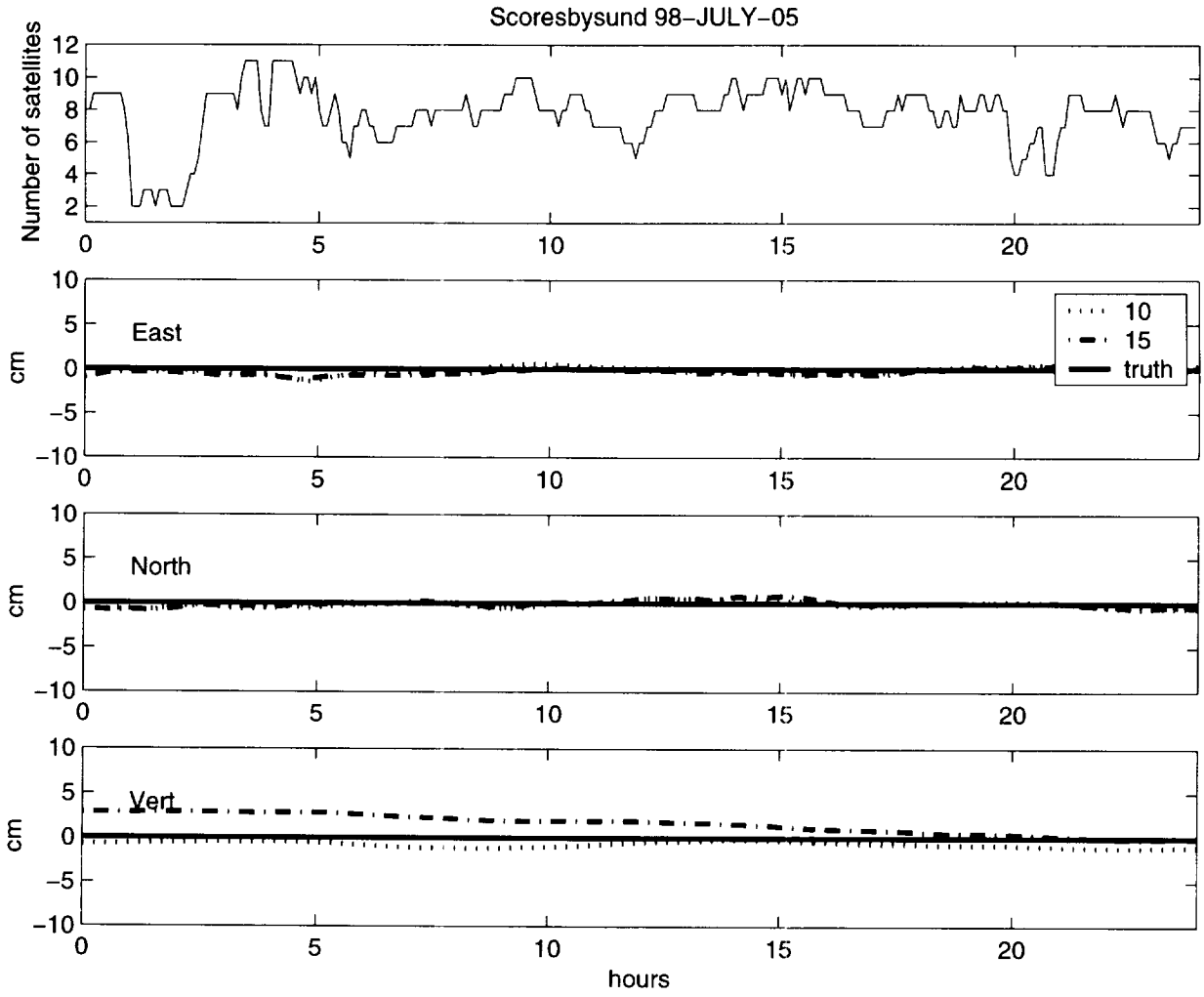

Figure 5. Residual receiver coordinates Scoresbysund, July 5, 1998. The *a priori* velocity has been removed, so that perfect agreement is shown at zero. Scoresbysund solutions are shown for elevation angle cut-offs of 10 and 15 degrees.

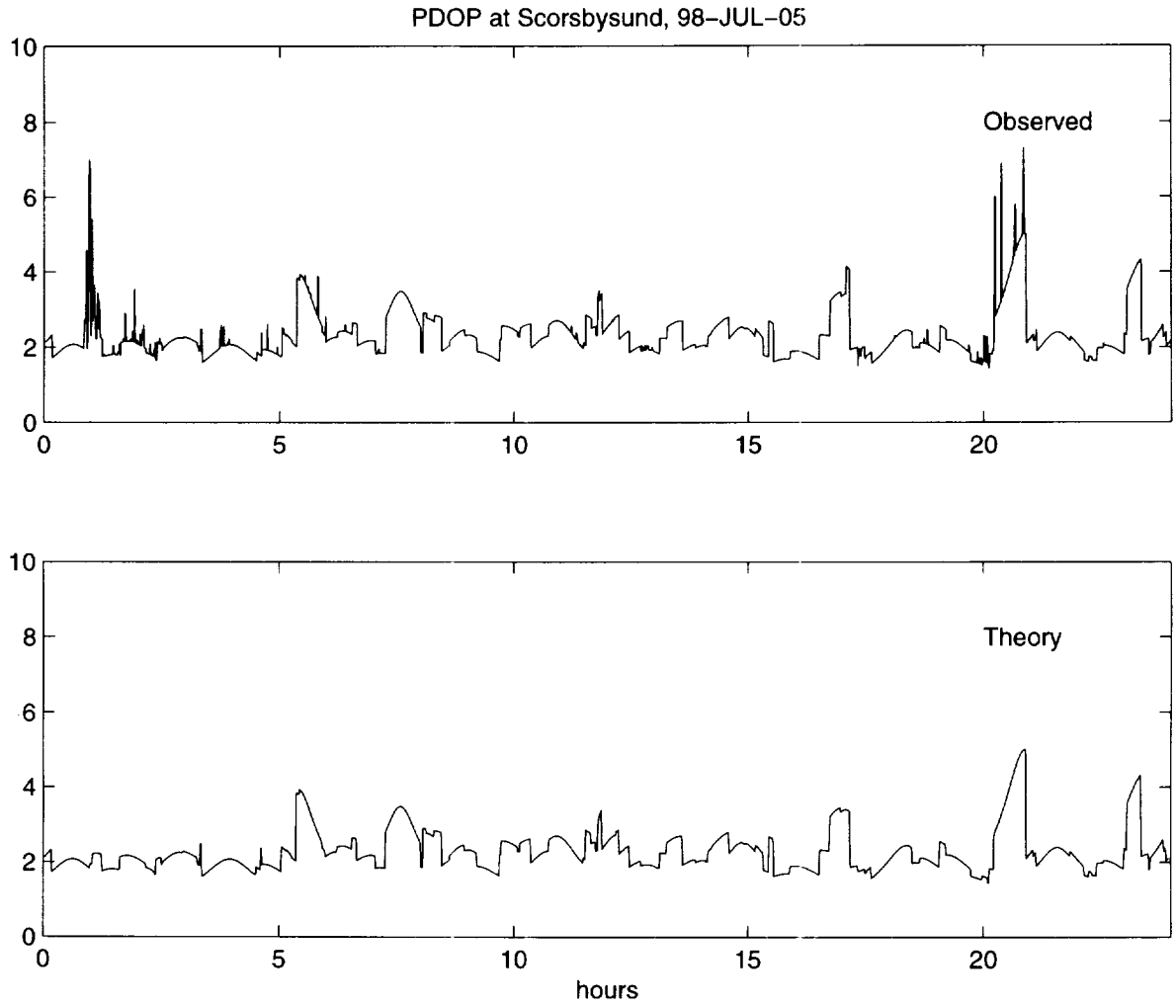

Figure 6. PODP at Scoresbysund, July 5, 1998.

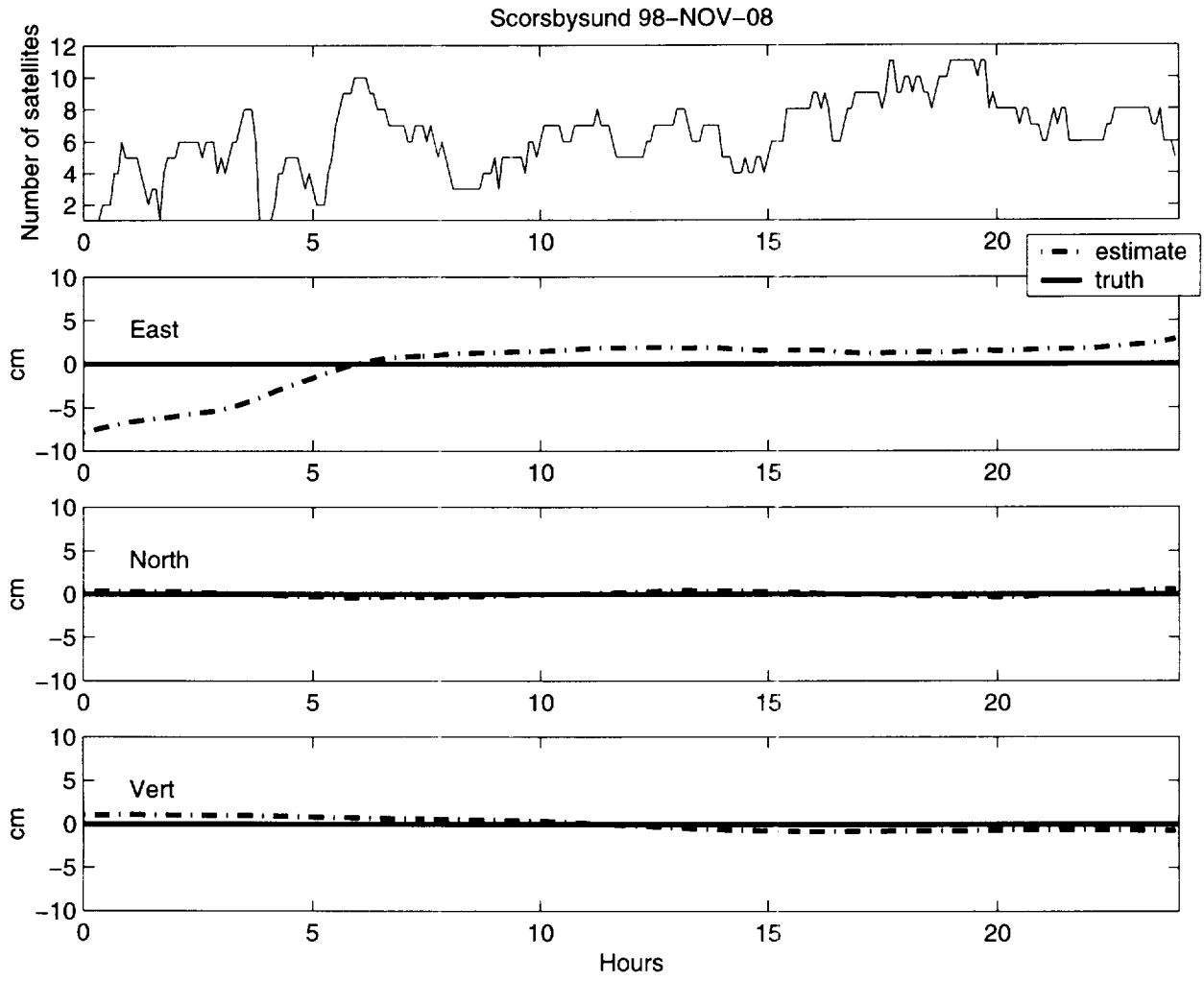

Figure 7. Residual receiver coordinates for Scoresbysund, November 8, 1998. The *a priori* velocity has been removed, so that perfect agreement is shown at zero.

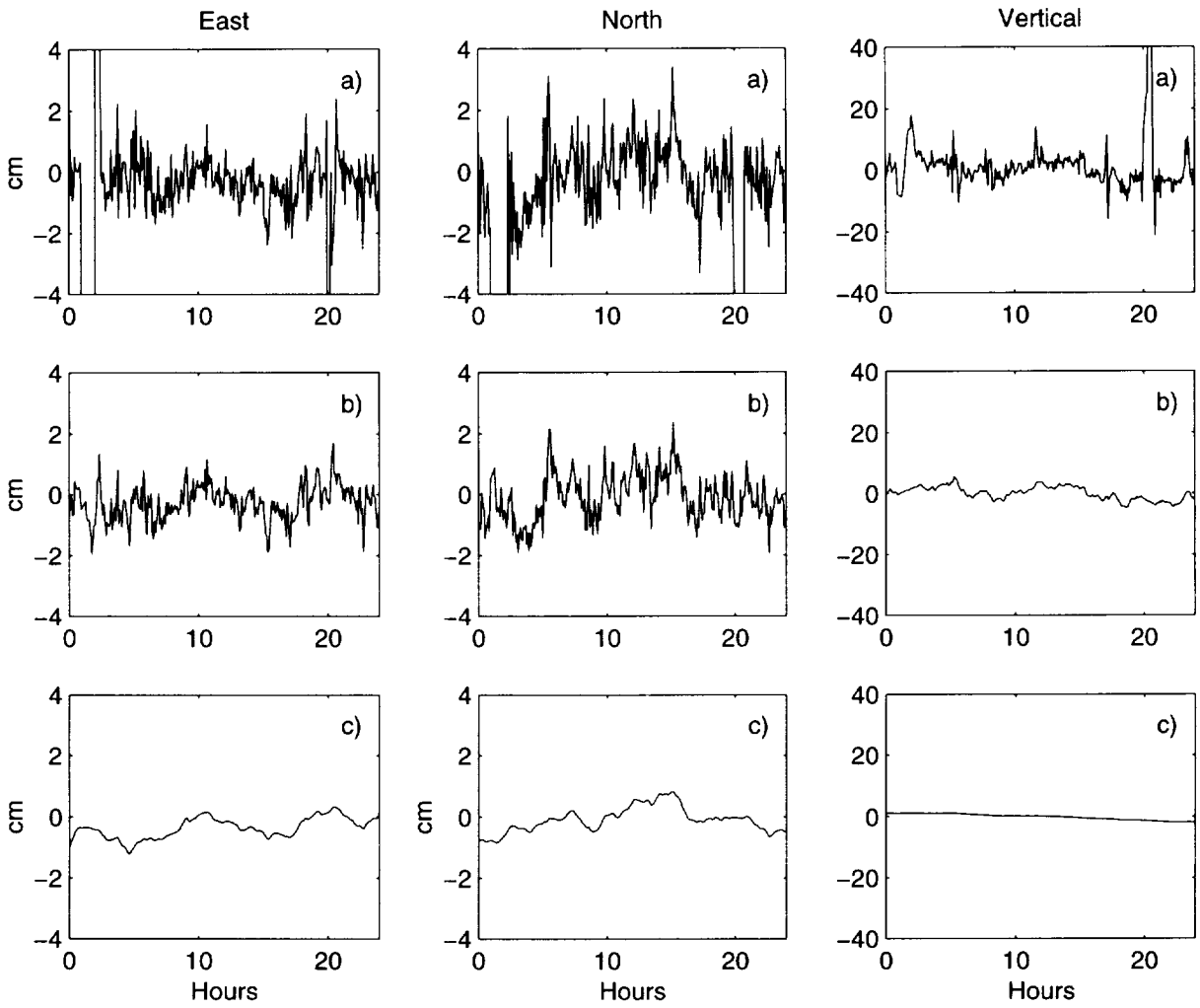

Figure 8. A comparison of filter strategies for Scoresbysund, July 5, 1998, white noise (a), and random walk σ_{rw} of 10^{-6} (b) and 10^{-7} (c) km/sqrt(sec). Note change in scale for the vertical component. In each case the true velocity is 0 cm/hr.

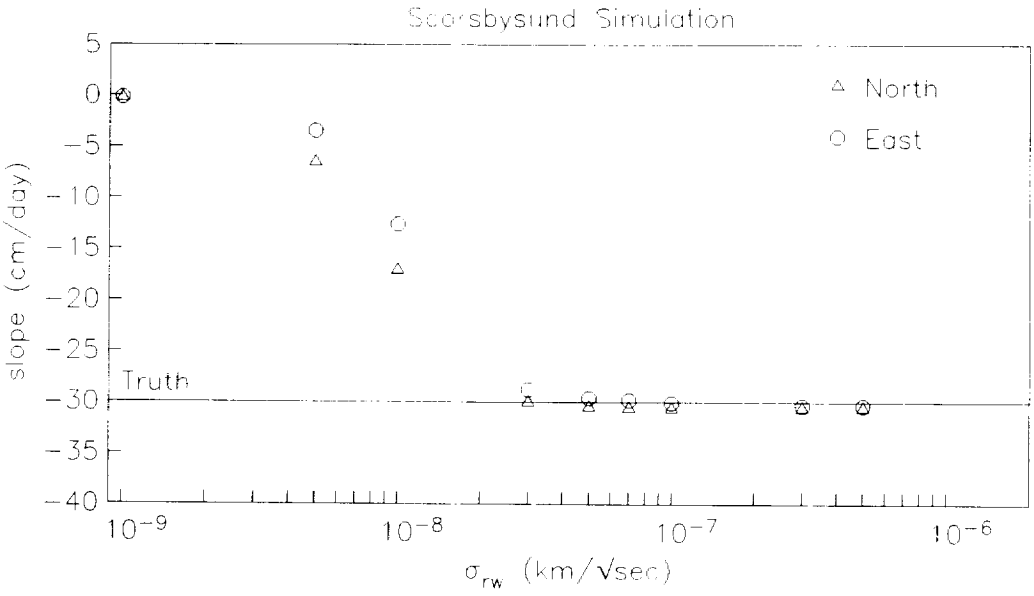

Figure 9. Comparison of solution velocities for various σ_{rw} for Scoresbysund, July 14, 1998.

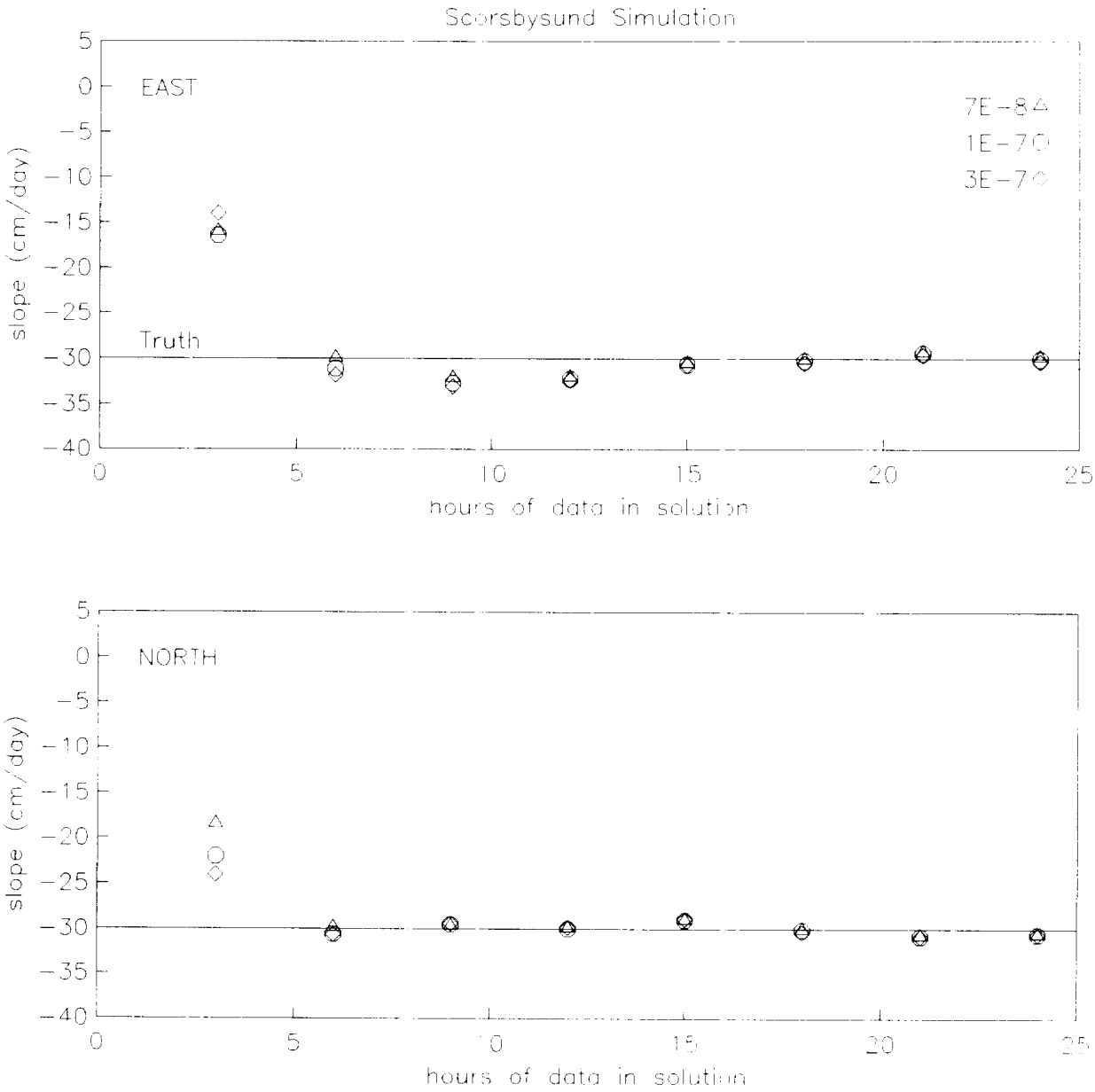

Figure 10. Comparison of solution velocities as a function of hours of data used in the solution; Scoresbysund, July 14, 1998.

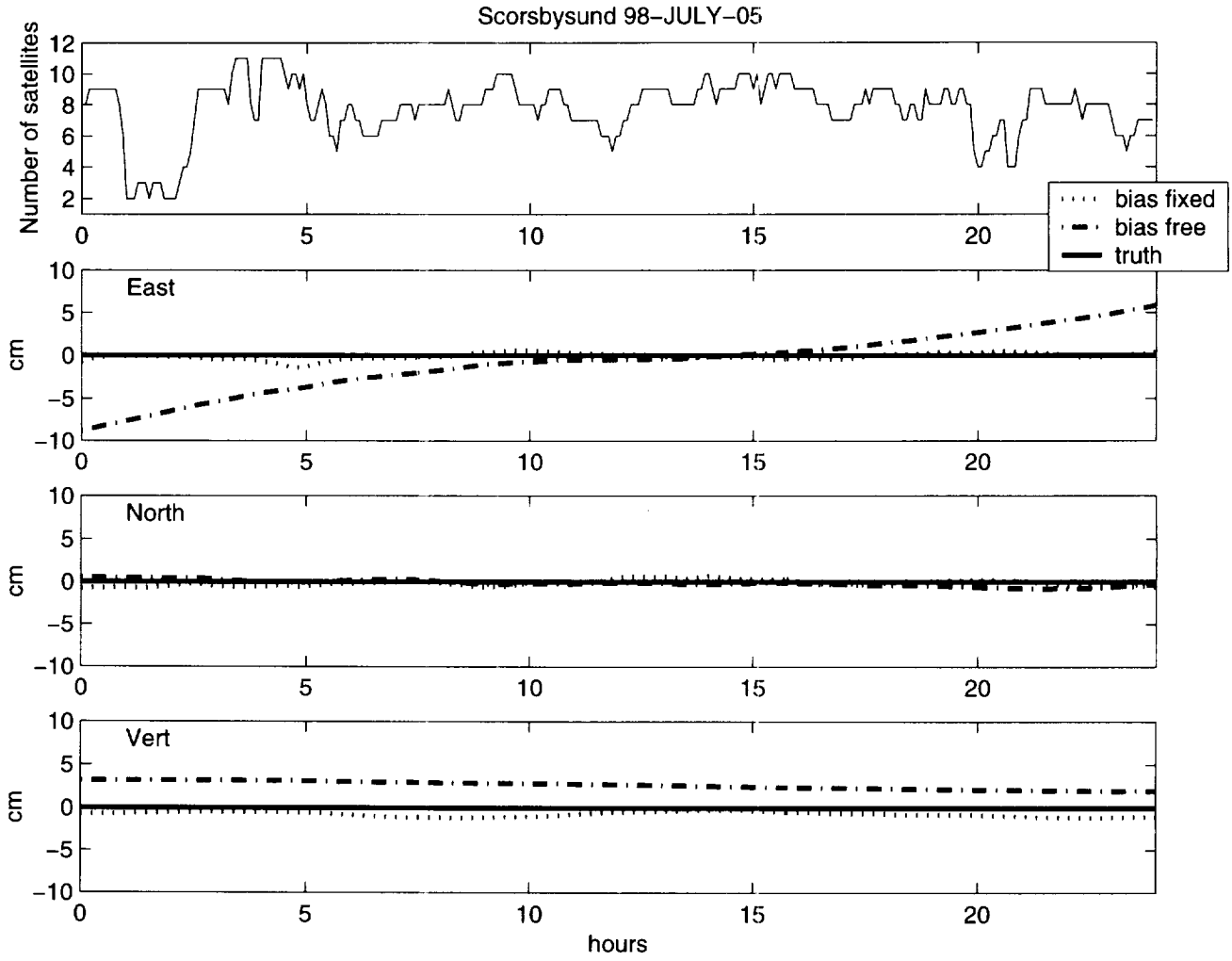

Figure 11. Comparison of bias fixed and bias free solution.

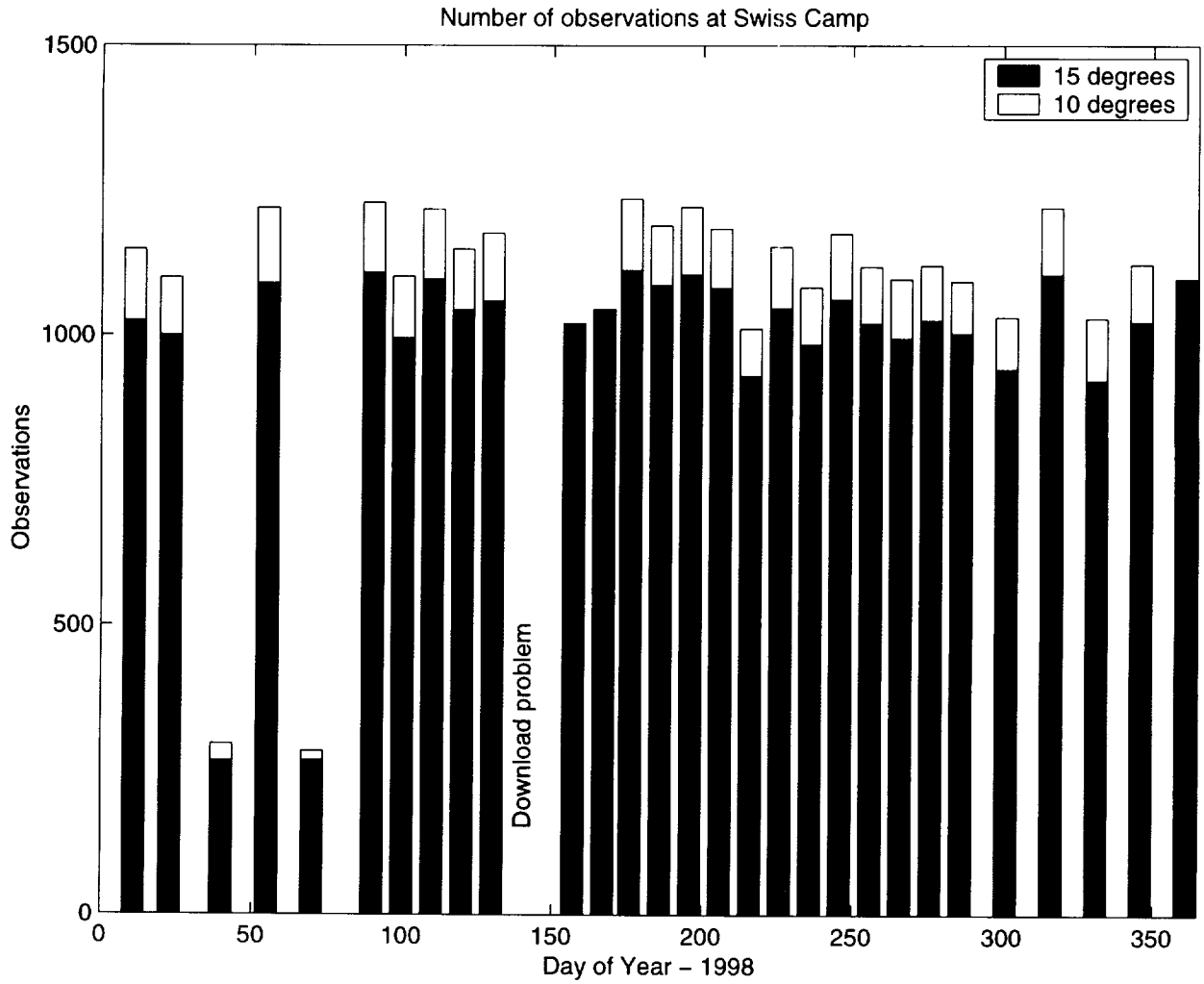

Figure 12. Number of observations above 10 and 15 degrees at Swiss Camp for 1998. Partially corrupted data files are seen for days 40 and 70; no data could be retrieved for day 146.

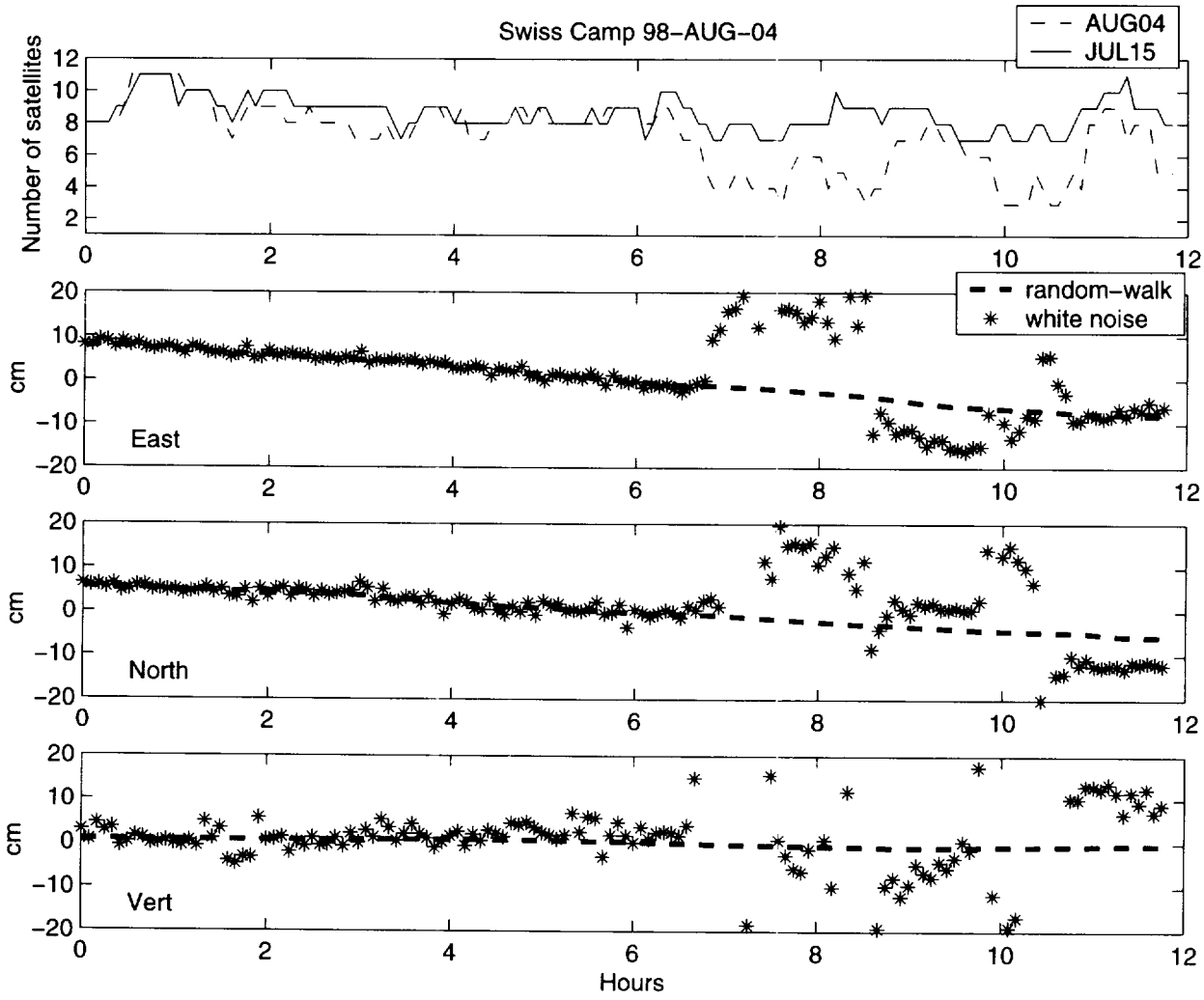

Figure 13. Comparison of Swiss Camp positions for August 4, 1998. Two filter solutions are shown, a random walk estimation with σ_{rw} of 10^{-7} and an unconstrained white noise solution. Note how the outliers in the white noise solution correlate with low number of GPS satellites on August 4. For comparison, the number of satellites visible on July 15 are also shown. An elevation cutoff of 10 degrees was used in both cases and ambiguities were resolved in each case.

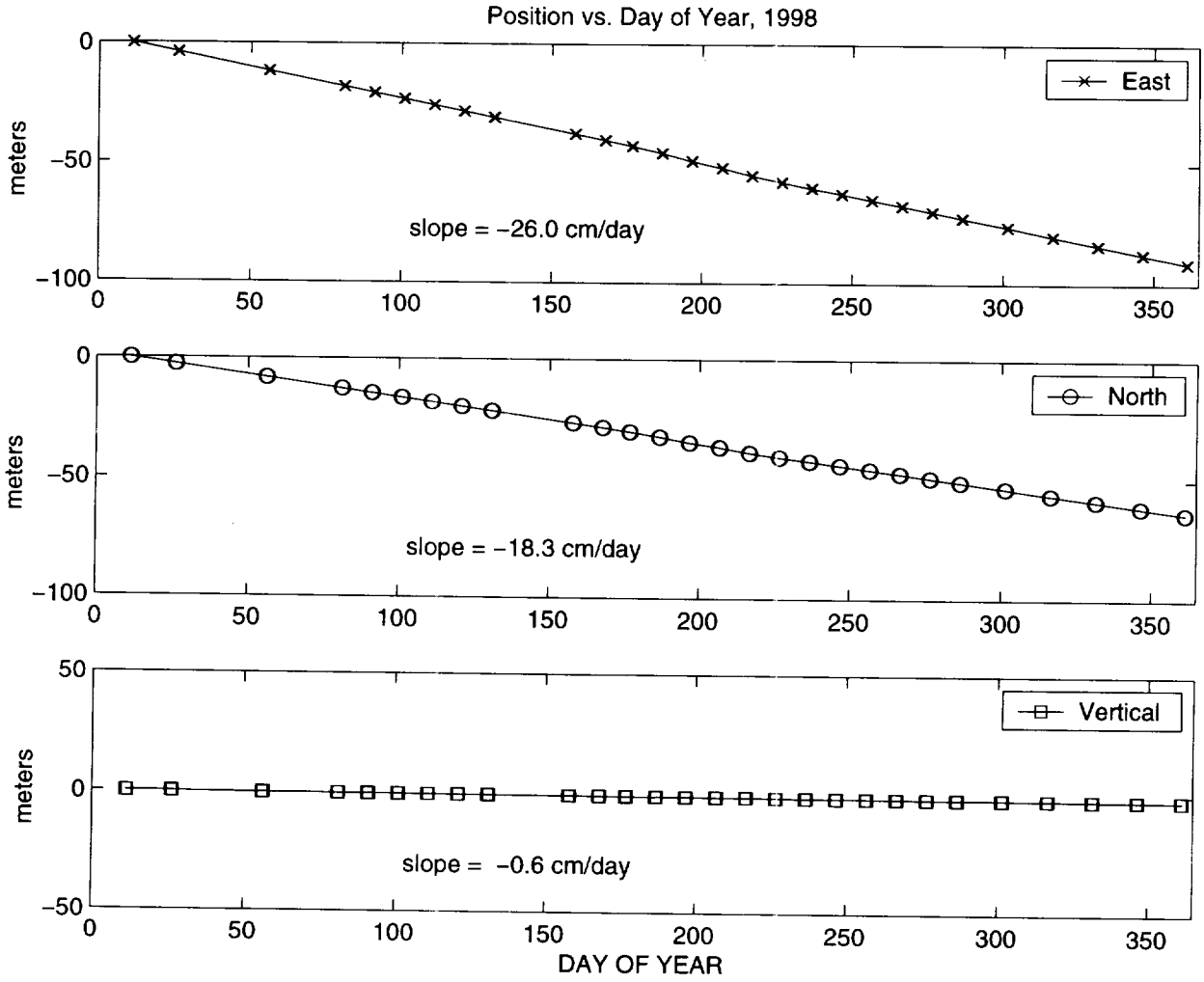

Figure 14. Estimates of the Swiss Camp position, rotated into local East, North, and Vertical directions. A best-fit straight-line is also shown.

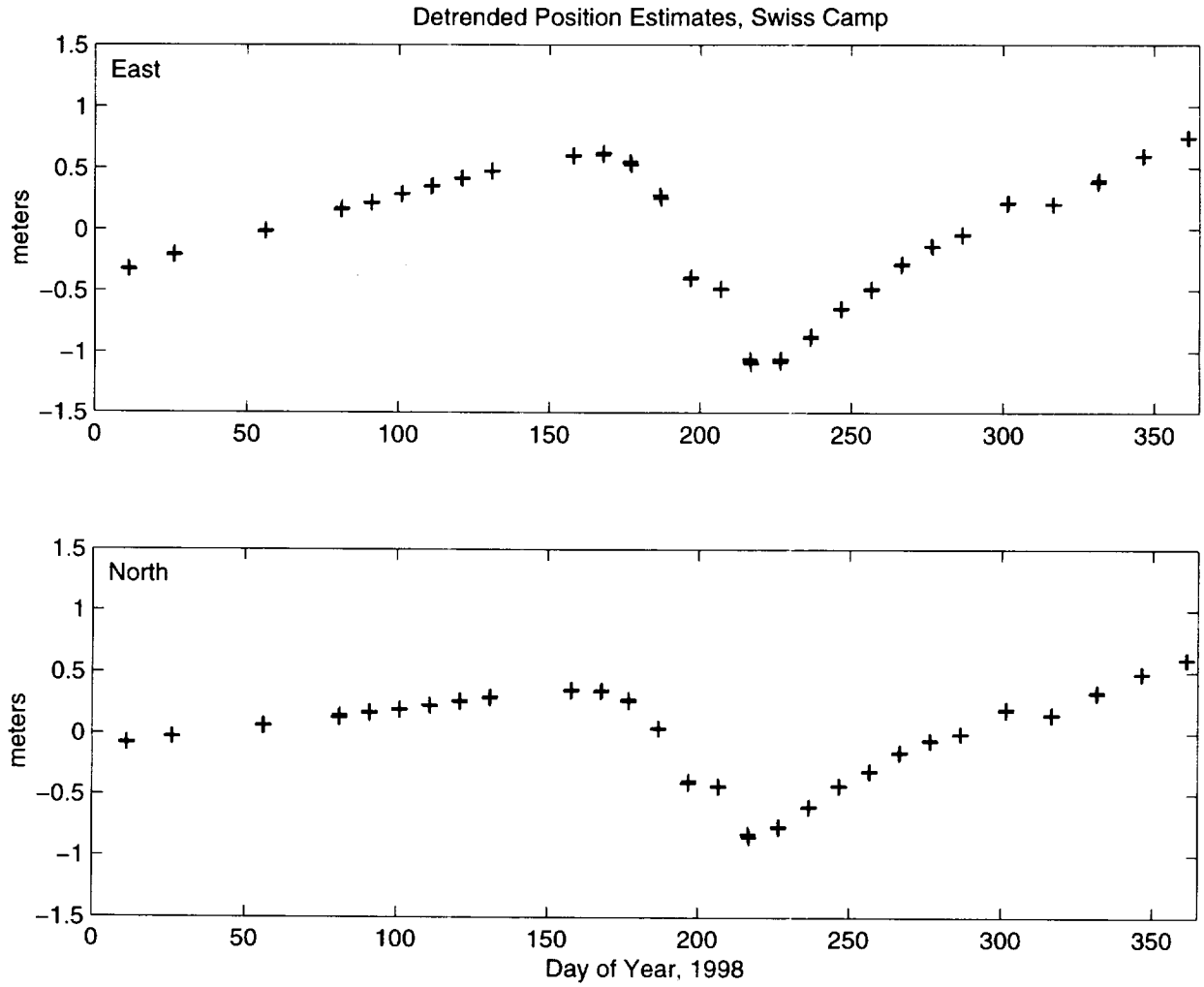

Figure 15. Detrended estimates of the Swiss Camp position, rotated into local East and North directions.

Table 1

Models	Values/Reference
Data interval	5 min
Elevation angle cut-off	10°
Geopotential	JGM3 degree and order 12
Precession	IAU 1976 precession theory
Nutation	IAU 1980 nutation theory
Earth Orientation	International Earth Rotation Service Bulletin B
Yaw attitude	[*Bar Sever*, 1996]
Ephemerides	IGS precise orbits, *Beutler et al.*, 1994
Reference clock	Thule
Pseudorange σ	100 cm
Carrier-phase σ	1 cm

Parameter	Estimation	Standard Deviation
Satellite clock	white noise	1 s
Receiver position, Swiss Camp	random walk	
Receiver clock	white noise	1 s
Phase ambiguity (real-valued)	constant	0.1 km
Zenith troposphere delay	random walk	1 cm/sqrt(hour)